Supporting Information (SI)

Efficient organic light-emitting diodes with narrow emission bandwidths based on iridium(III) complexes with pyrido[3',2':4,5]pyrrolo[3,2,1-*jk*]carbazole unit

Xiang-Ji Liao[1#], Jin-Jun Zhu[1#], Li Yuan[1], Zhi-Ping Yan[1], Zhen-Long Tu[1], Meng-Xi Mao[1], Jun-Jian Lu[1], Wen-Wei Zhang[1*] and You-Xuan Zheng[1,2*]

[1]State Key Laboratory of Coordination Chemistry, Jiangsu Key Laboratory of Advanced Organic Materials, School of Chemistry and Chemical Engineering, Nanjing University, Nanjing 210093, China. E-mail: yxzheng@nju.edu.cn, wwzhang@nju.edu.cn

#Liao and Zhu have same contribution to this paper.

S1. General information

NMR measurements were conducted on a Bruker AM 400 spectrometer. High resolution electrospray mass spectra (HRMS) was measured on G6500 from Agilent for complexes. Absorption spectra were measured on a UV-3100 spectrophotometer and photoluminescence spectra were obtained from a Hitachi F-4600 photoluminescence spectrophotometer. Cyclic voltammetry measurements were conducted on a MPI-A multifunctional electrochemical and chemiluminescent system (Xi'an Remex Analytical Instrument Ltd. Co., China) at room temperature, with a polished Pt plate as the working electrode, platinum thread as the counter electrode and Ag-AgNO$_3$ (0.1 M) in CH$_3$CN as the reference electrode, tetra-*n*-butylammonium perchlorate (0.1 M) was used as the supporting electrolyte, using Fc$^+$/Fc as the external standard, the scan rate was 0.1 V/s. HOMO energy was calculated from the oxidation potential with the formula of HOMO = -[E_{ox} - $E_{(Fc/Fc+)}$ + 4.8] eV. The energy gap (E_g) of HOMO and LUMO was calculated from the onset of the absorption spectrum with the formula of E_g, = 1240 / λ_{onset} and LUMO energy was calculated from HOMO - E_g. The absolute photoluminescence quantum yields (Φ) and the decay lifetimes of the compounds was measured with HORIBA FL-3 fluorescence spectrometer. Thermogravimetric analysis (TGA) was performed on a Pyris 1 DSC under nitrogen at a heating rate of 10 ℃ min^{-1} .The single crystals of complexes were carried out on a Bruker SMART CCD diffractometer using monochromated Mo Ka radiation (λ = 0.71073 Å) at room temperature. Cell parameters were retrieved using SMART software and refined using SAINT on all observed reflections. HPLC Analysis

Conditions: a) Column: Cat. No. EnantioPak®Y7, 5μm, 250 × 30 mm; b) Mobile phase: n-Hexane/Ethanol = 60/40(v/v); c) Flow rate: 24.0 mL/min; d) Abs. detector: 254 nm.

S2. OLEDs fabrication and measurement.

All OLEDs were fabricated on the pre-patterned ITO-coated glass substrate with a sheet resistance of 15 Ω sq^{-1}. The deposition rate for organic compounds is 1-2 Å s^{-1}. The phosphor and the host (2,6DCzPPy) was co-evaporated to form emitting layer from two separate sources. The cathode consisting of LiF / Al was deposited by evaporation of LiF with a deposition rate of 0.1 Å s^{-1} and then by evaporation of Al metal with a rate of 3 Å s^{-1}. The characteristic curves of the devices were measured with a computer which controlled KEITHLEY 2400 source meter with a calibrated silicon diode in air without device encapsulation. On the basis of the uncorrected PL and EL spectra, the Commission Internationale de l'Eclairage (CIE) coordinates were calculated using a test program of the Spectra scan PR650 spectrophotometer, The EQE of EL devices were calculated based on the photo energy measured by the photodiode.
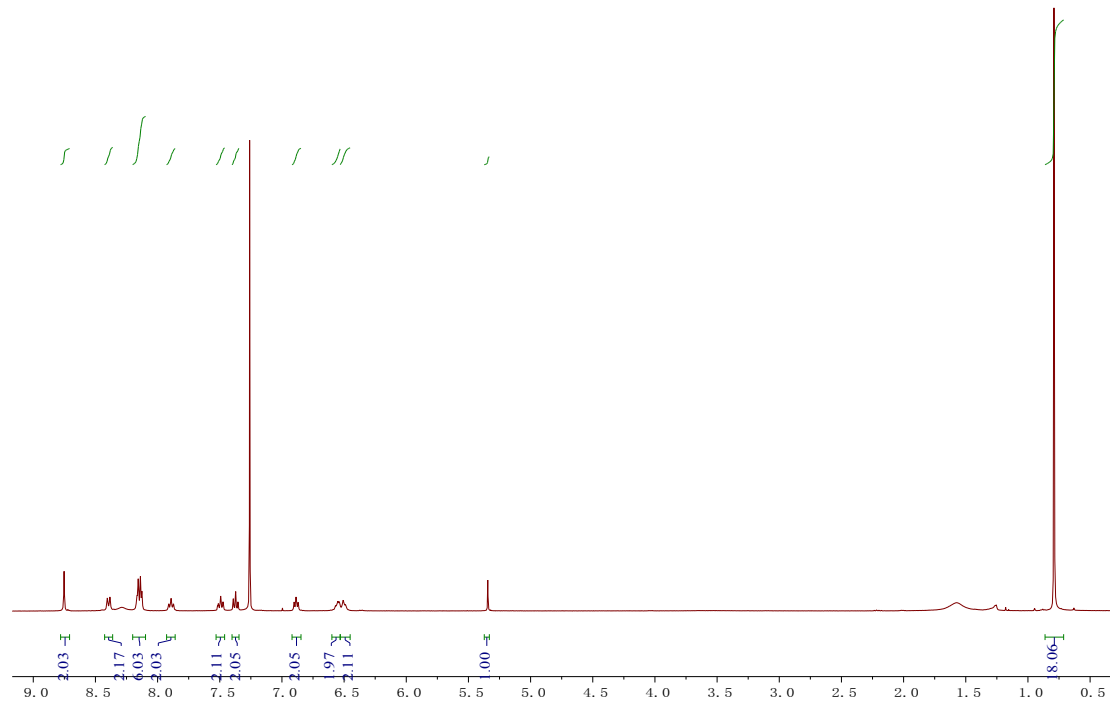

Fig. S1. ^{1}H NMR spectrum of Ir1.
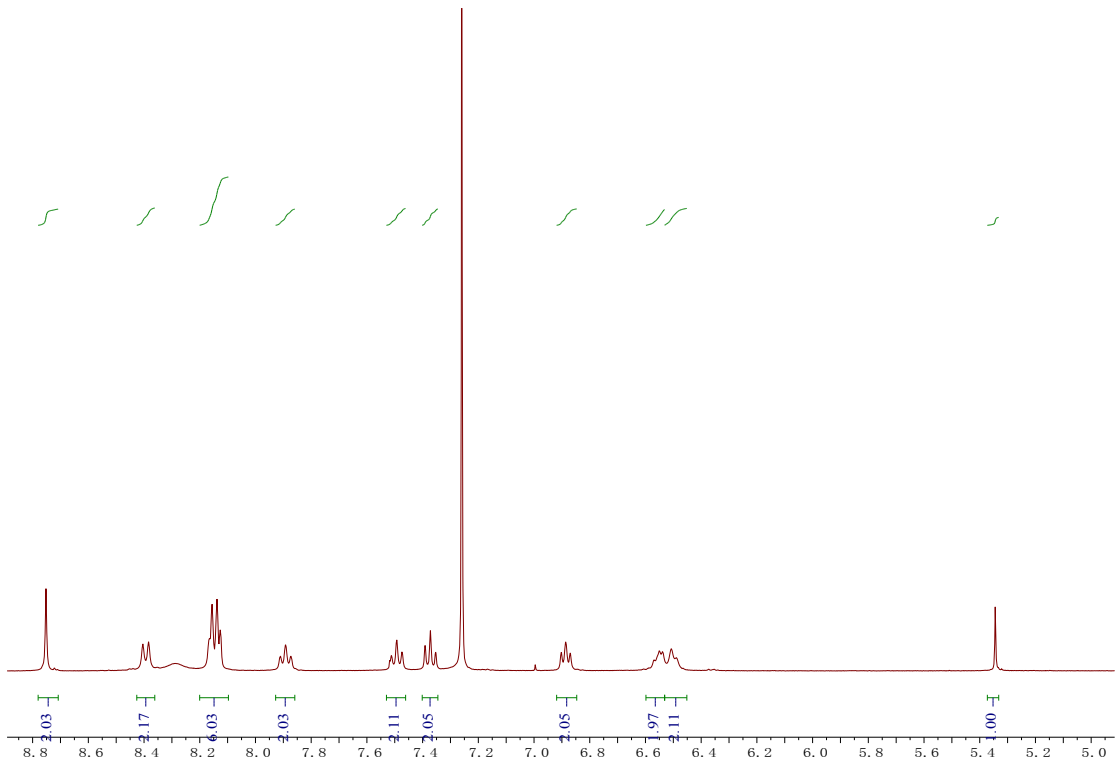
**Fig. S2.** ¹H NMR Zoomed spectrum in 5-9 ppm regions of Ir1.
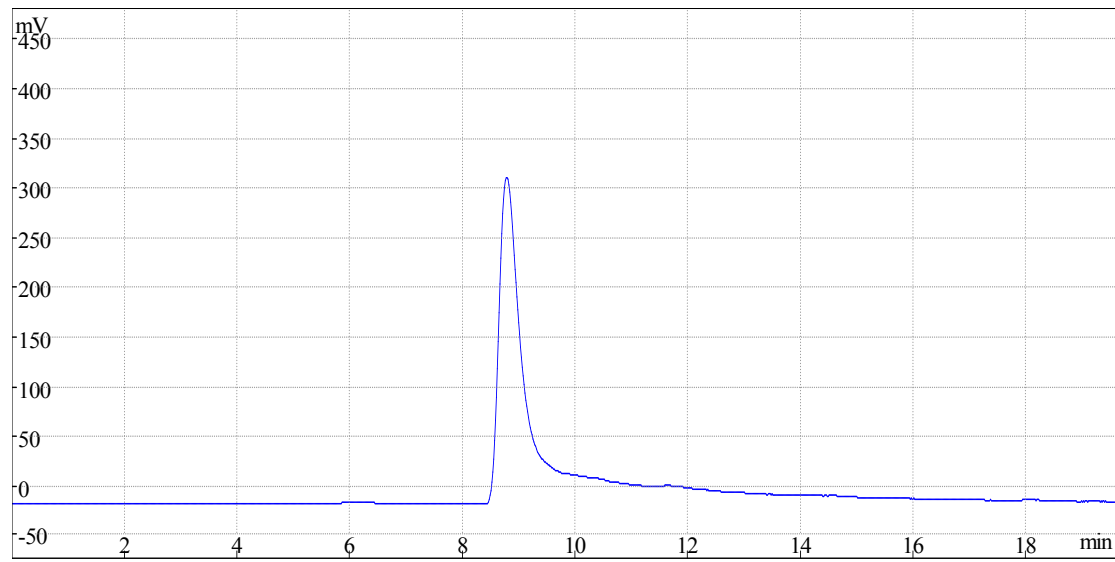
**Fig. S3.** HPLC profile of Ir1.
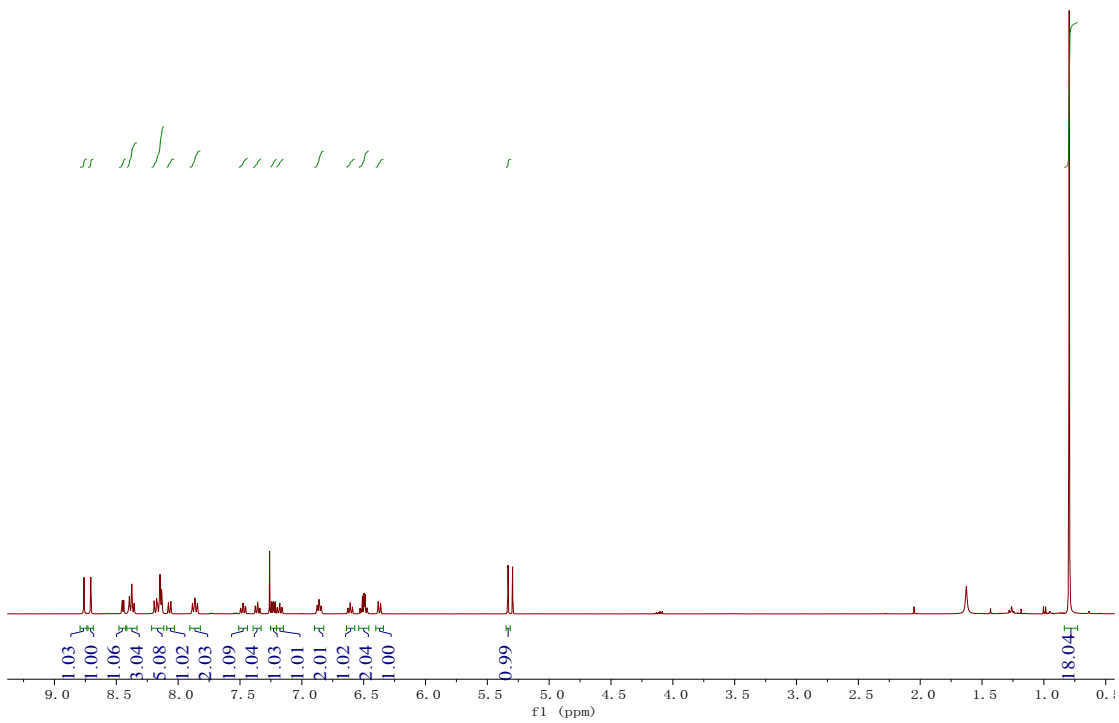
**Fig. S4.** ^{1}H NMR spectrum of Ir2.
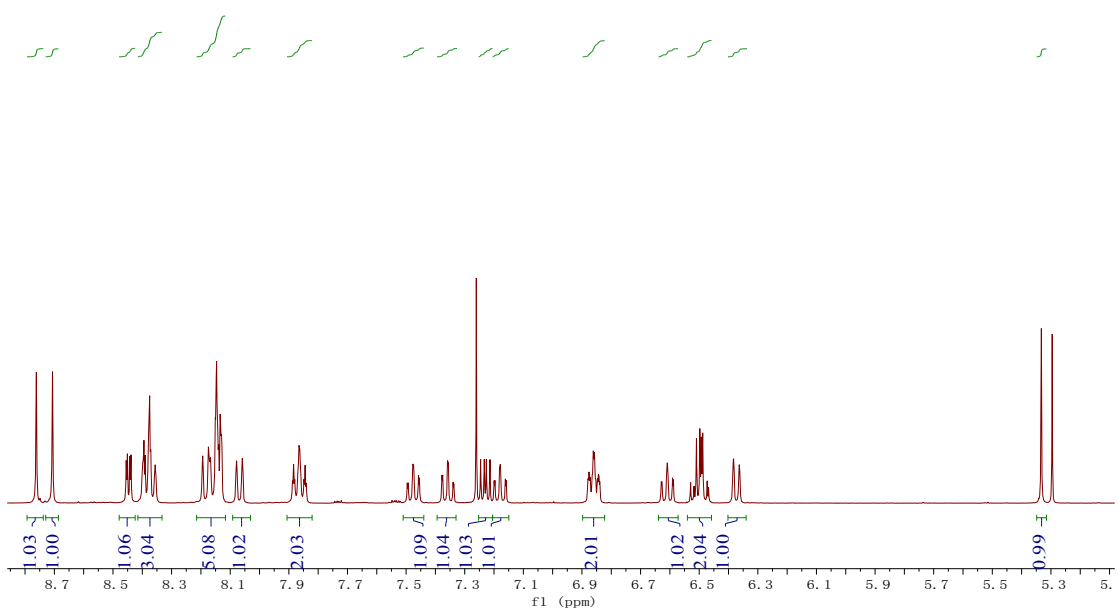
**Fig. S5.** ^{1}H NMR Zoomed spectrum in 5-9 ppm regions of Ir2.

4
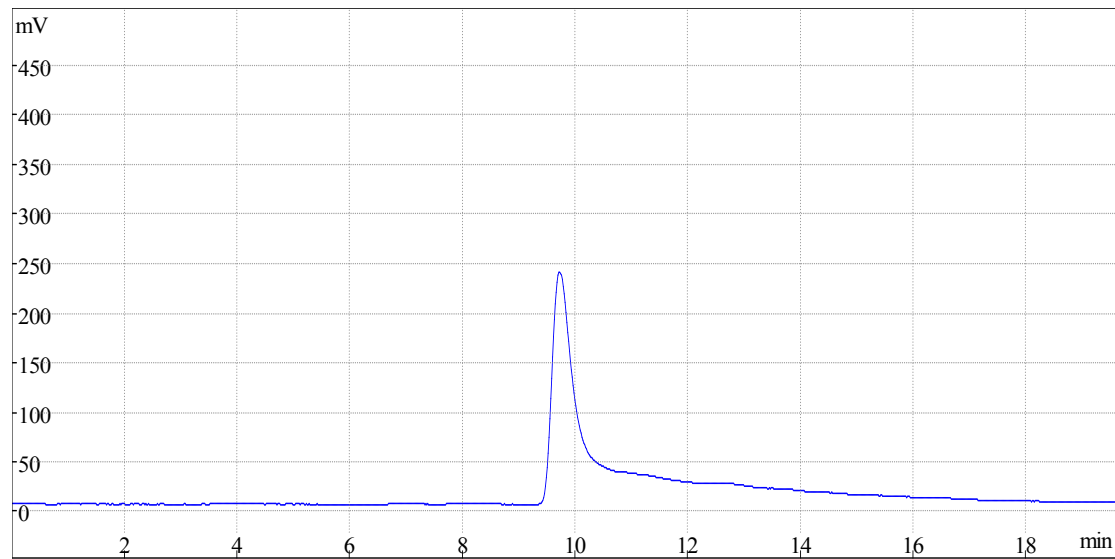
Fig. S6. HPLC profile of Ir2.
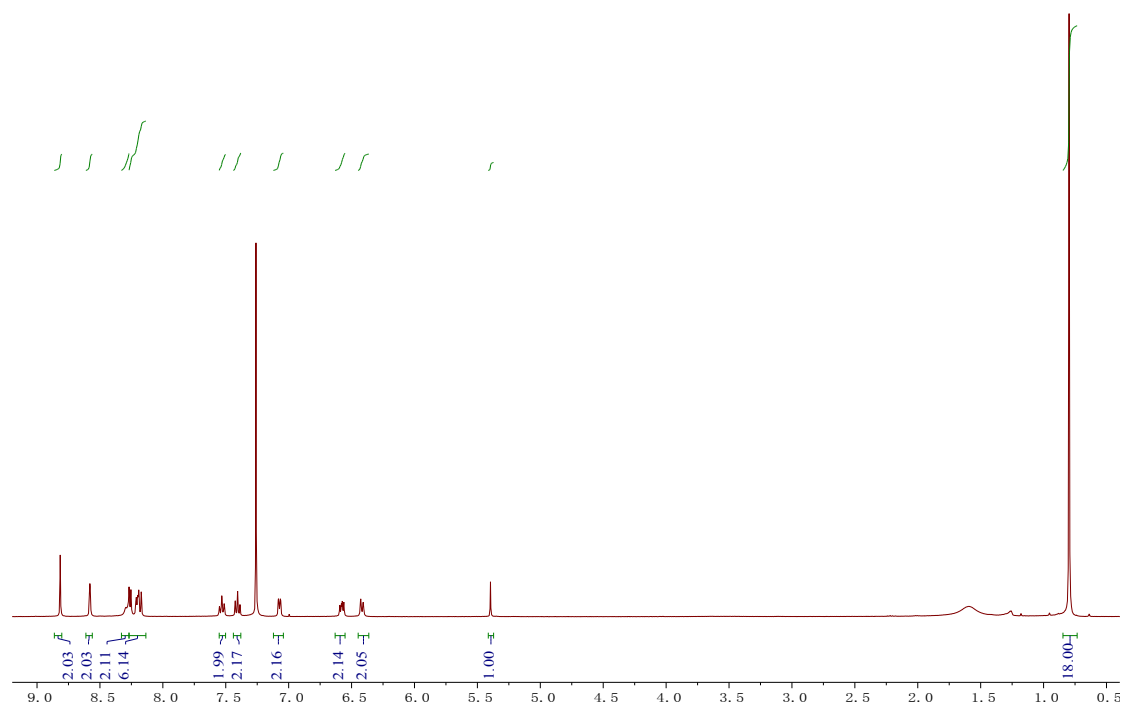
Fig. S7. ^{1}H NMR spectrum of Ir3.
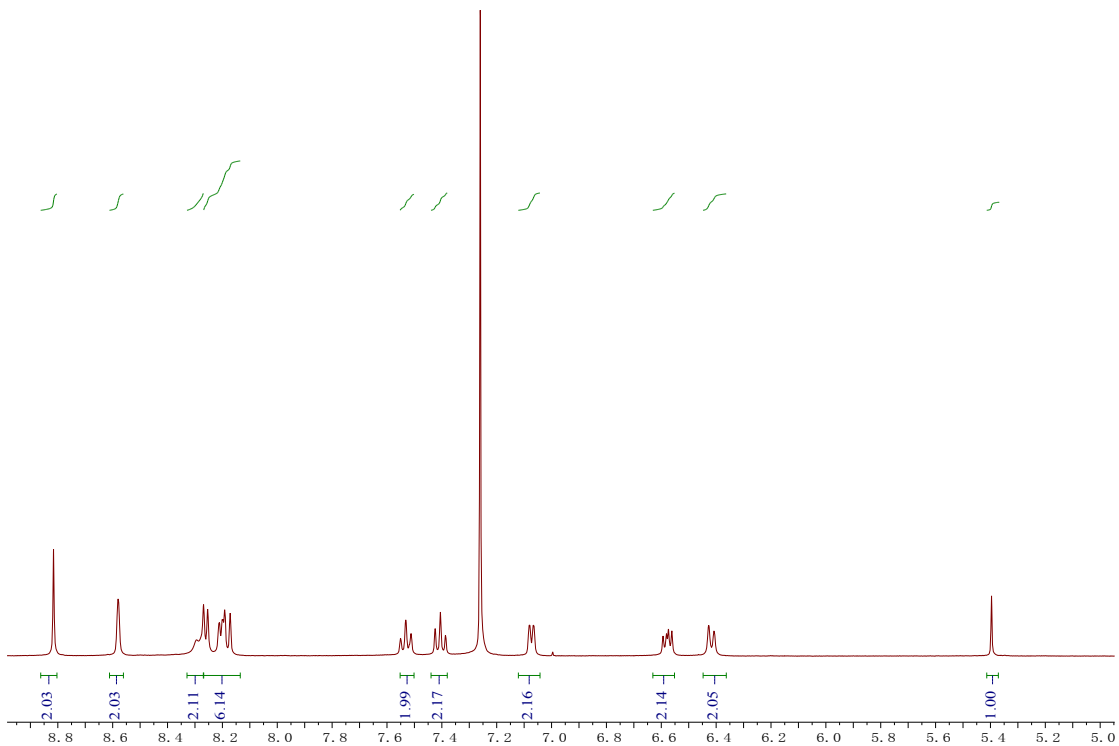
Fig. S8. ^{1}H NMR Zoomed spectrum in 5-9 ppm regions of Ir3.
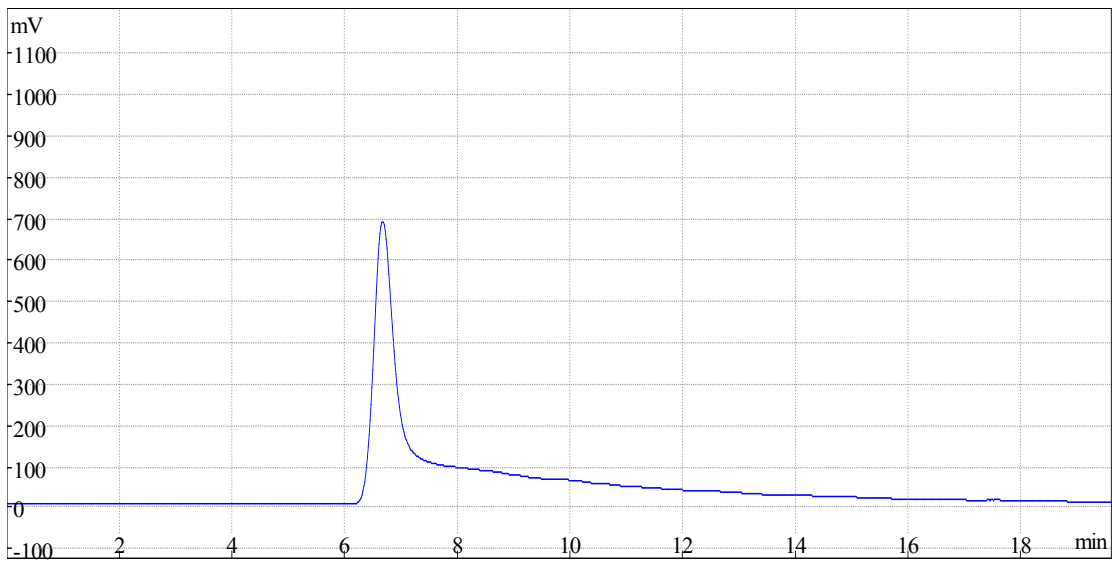
**Fig. S9.** HPLC profile of Ir3.

6
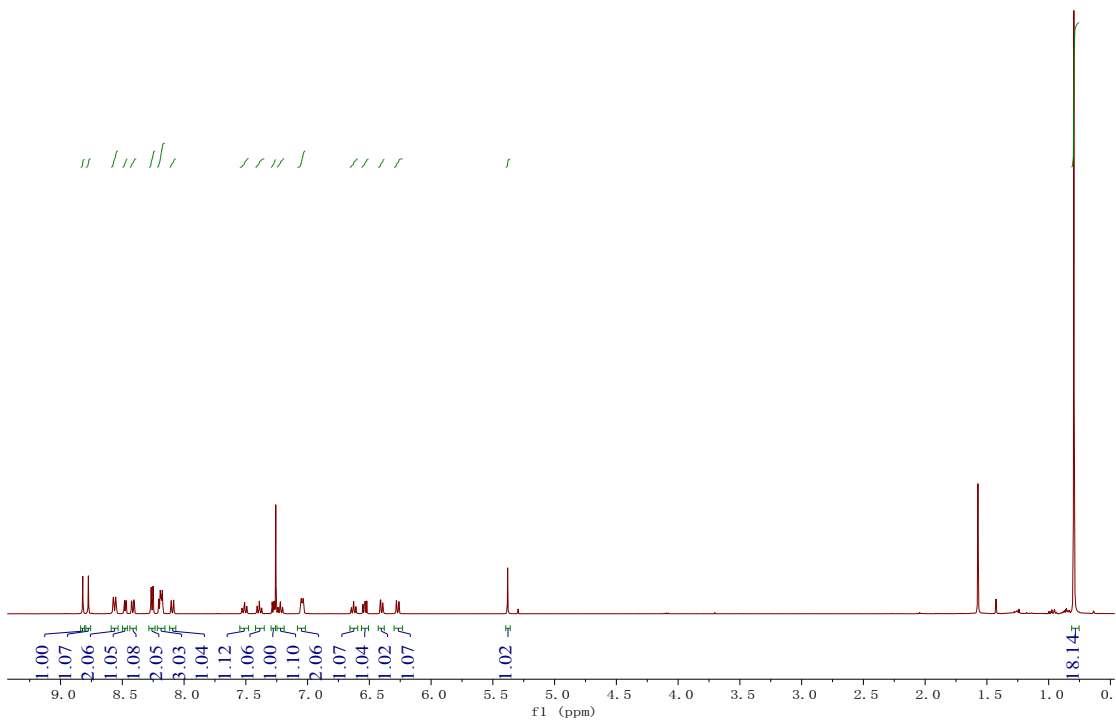
**Fig. S10.** ^{1}H NMR spectrum of Ir4.
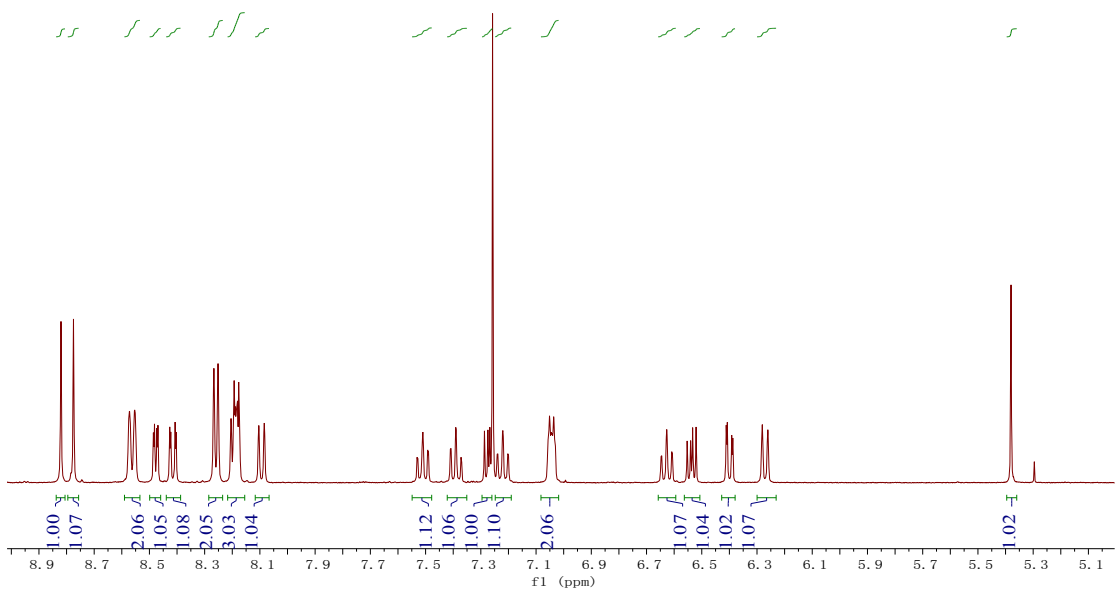
**Fig. S11.** ^{1}H NMR Zoomed spectrum in 5-9 ppm regions of Ir4.
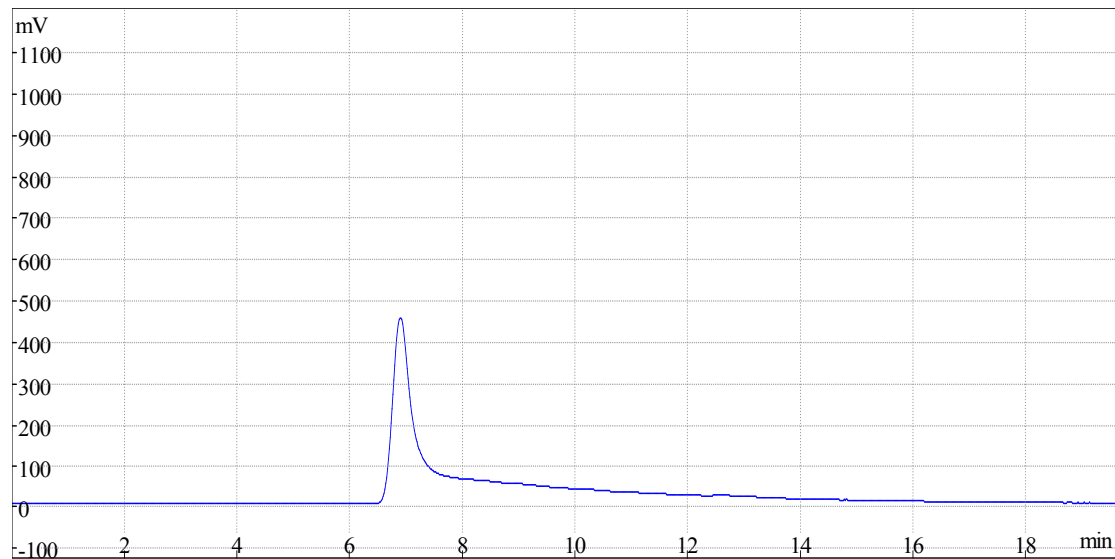
Fig. S12. HPLC profile of Ir4.
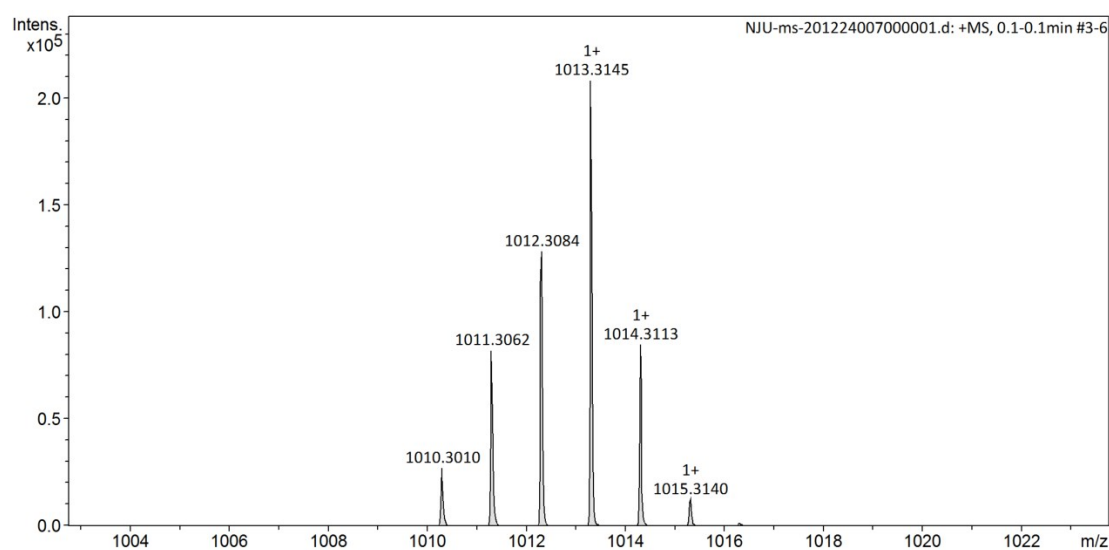


Fig. S13. HRMS spectrum of Ir1.
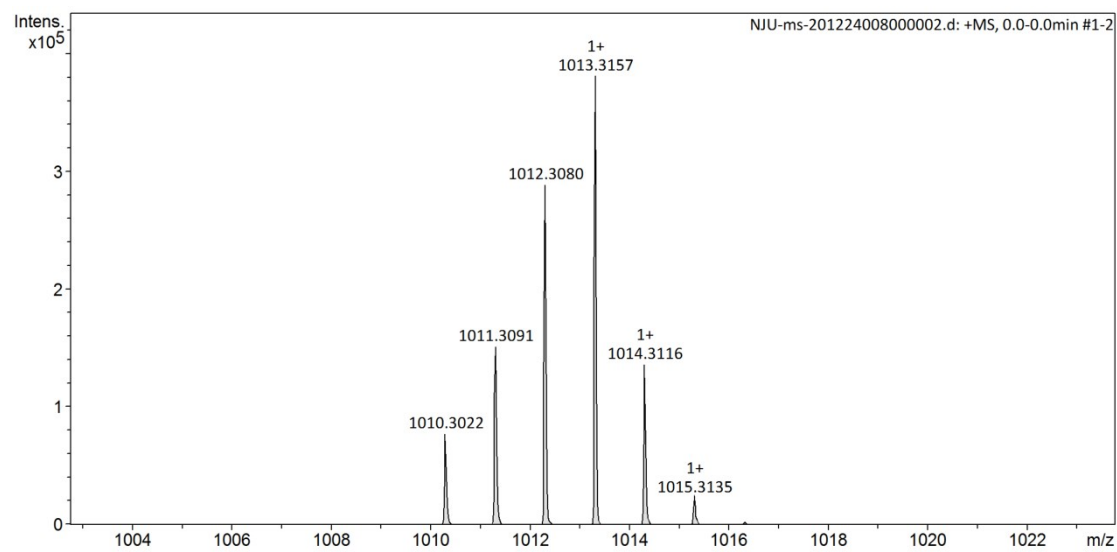
Fig. S14. HRMS spectrum of Ir2.
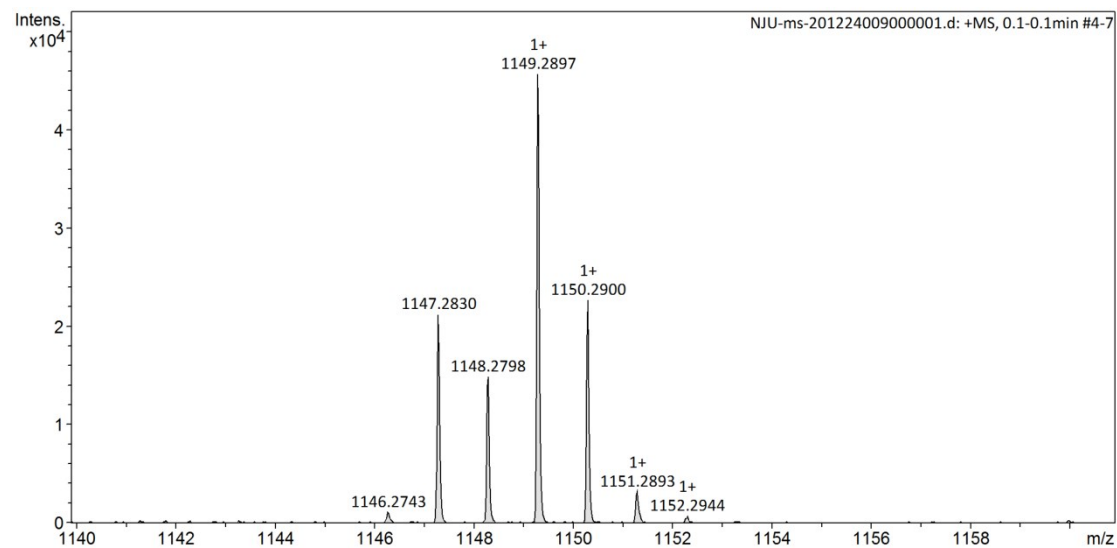
Fig. S15. HRMS spectrum of Ir3.
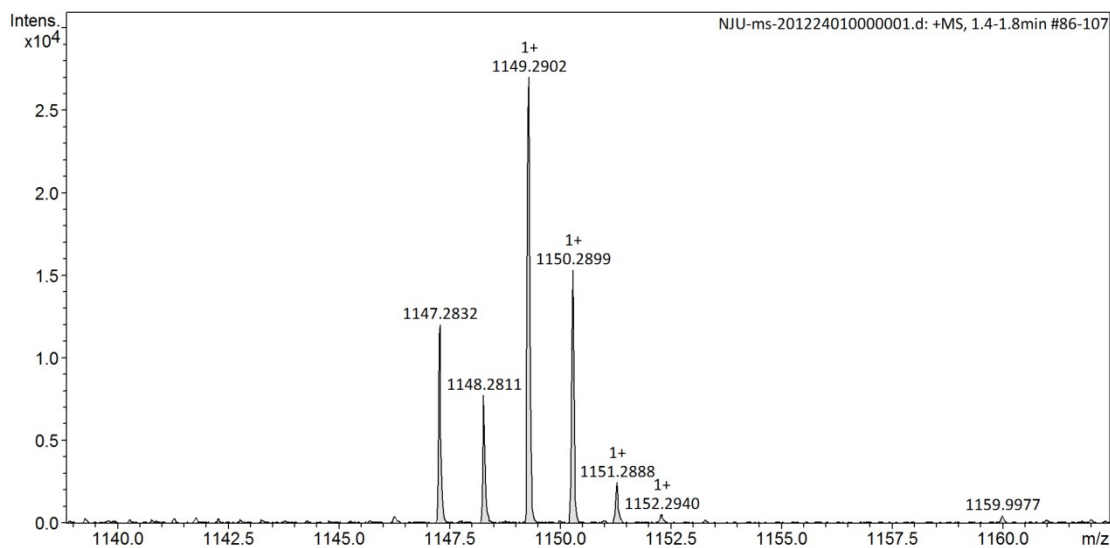
Fig. S16. HRMS spectrum of Ir4.

Table S1. Crystal information of Ir1 and Ir2.

	Ir1	Ir2
Formula	$C_{55}H_{43}IrN_6O_2$	$C_{55}H_{43}IrN_6O_2$
Formula weight	1012.15	1012.15
T (K)	193.01	193.0
Wavelength (Å)	1.34139	1.34139
Crystal system	Monoclinic	Monoclinic
Space group	$P2_1/n$	$P2_1/n$
a (Å)	12.9988(5)	15.1656(11)
b (Å)	17.4052(7)	17.0198(13)
c (Å)	19.7083(7)	19.2841(15)
α (deg)	90	90
β (deg)	90.2110(10)	103.456(2)
γ (deg)	90	90
V (Å^3)	4458.9(3)	4840.9(6)
Z	4	4
ρ_{calcd} (mg m^{-3})	1.508	1.389
μ (Mo Kα) (mm^{-1})	4.277	3.940
F (000)	2032	2032
Reflns collected	33035	33828
Unique	8093	8828
Data/restraints/params	8093 / 0 / 583	8828/78/614
GOF on F^2	1.080	1.035

$R_1{}^a$, $wR_2{}^b$[$I > 2\sigma(I)$]	0.0239,0.0657	0.0258,0.0666
$R_1{}^a$, $wR_2{}^b$(all data)	0.0255, 0.0668	0.0289, 0.0684
CCDC NO	2052176	2052164

$R_1{}^a = \sum||F_o|-|F_c||/\sum|F_o|$. $wR_2{}^b = [\sum w(F_o{}^2-F_c{}^2)^2/\sum w(F_o{}^2)]^{1/2}$

Table S2. Selected bond lengths and angles of Ir1.

Selected bonds (Å)			
Ir(01)-O(002)	2.1555(17)	Ir(01)-O(003)	2.1170(17)
Ir(01)-N(004)	2.018(2)	Ir(01)-N(005)	2.037(2)
Ir(01)-C(00A)	1.993(2)	Ir(01)-C(00C)	1.988(3)

Selected angles (°)			
O(003)-Ir(01)-O(002)	87.57(7)	N(004)-Ir(01)-O(002)	85.25(7)
N(004)-Ir(01)-O(003)	91.62(8)	N(004)-Ir(01)-N(005)	173.22(8)
N(005)-Ir(01)-O(002)	91.40(8)	N(005)-Ir(01)-O(003)	82.34(7)
C(00A)-Ir(01)-O(002)	89.41(8)	C(00A)-Ir(01)-O(003)	172.20(8)
C(00A)-Ir(01)-N(004)	80.96(9)	C(00A)-Ir(01)-N(005)	104.94(9)
C(00C)-Ir(01)-O(002)	171.73(9)	C(00C)-Ir(01)-O(003)	88.84(8)
C(00C)-Ir(01)-N(004)	102.30(9)	C(00C)-Ir(01)-N(005)	80.74(9)
C(00C)-Ir(01)-C(00A)	95.05(10)		

Table S3. Selected bond lengths and angles of Ir2.

Selected bonds (Å)			
Ir(01)-O(002)	2.1117(18)	Ir(01)-O(003)	2.1364(18)
Ir(01)-N(004)	2.025(2)	Ir(01)-N(005)	2.026(2)
Ir(01)-C(00A)	1.989(3)	Ir(01)-C(00C)	2.002(3)

Selected angles (°)			
O(002)-Ir(01)-O(003)	87.75(7)	N(004)-Ir(01)-O(002)	92.96(8)
N(004)-Ir(01)-O(003)	82.49(8)	N(004)-Ir(01)-N(005)	174.53(9)
N(005)-Ir(01)-O(002)	82.53(8)	N(005)-Ir(01)-O(003)	94.19(8)
C(00A)-Ir(01)-O(002)	84.31(9)	C(00A)-Ir(01)-O(003)	171.16(9)
C(00A)-Ir(01)-N(004)	101.77(10)	C(00A)-Ir(01)-N(005)	80.94(10)
C(00A)-Ir(01)-C(00C)	99.82(10)	C(00C)-Ir(01)-O(002)	173.22(9)
C(00C)-Ir(01)-O(003)	88.46(9)	C(00C)-Ir(01)-N(004)	80.98(10)

C(00C)-Ir(01)-N(005)   103.35(10)

Table S4. HOMO and LUMO electron cloud density distributions of each fragment of two Ir(III) complexes.

Complex	Orbital	Energy/ eV	E_g/ eV	Composition (%)		
				Ir	Main ligand	Ancillary ligand
Ir1	HOMO	-5.04	3.54	37.17	58.80	4.03
	LUMO	-2.50		3.31	91.91	4.78
Ir3	HOMO	-5.33	2.70	32.24	63.17	4.59
	LUMO	-2.63		2.14	92.67	5.19
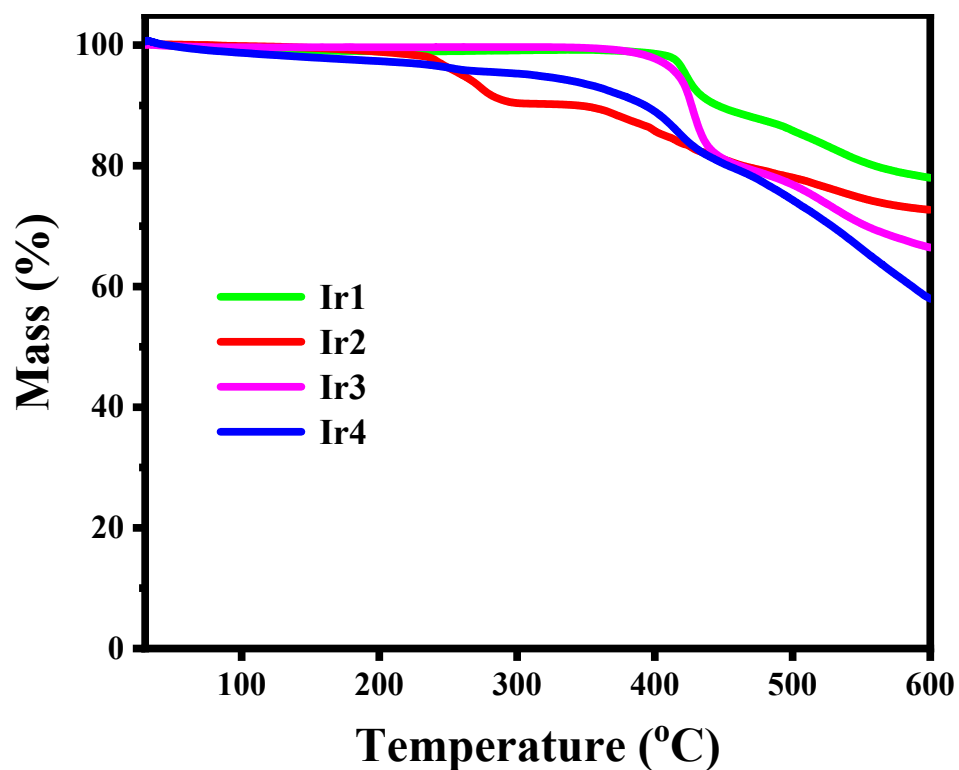
Fig. S17. TGA curves of Ir1-Ir4.

12
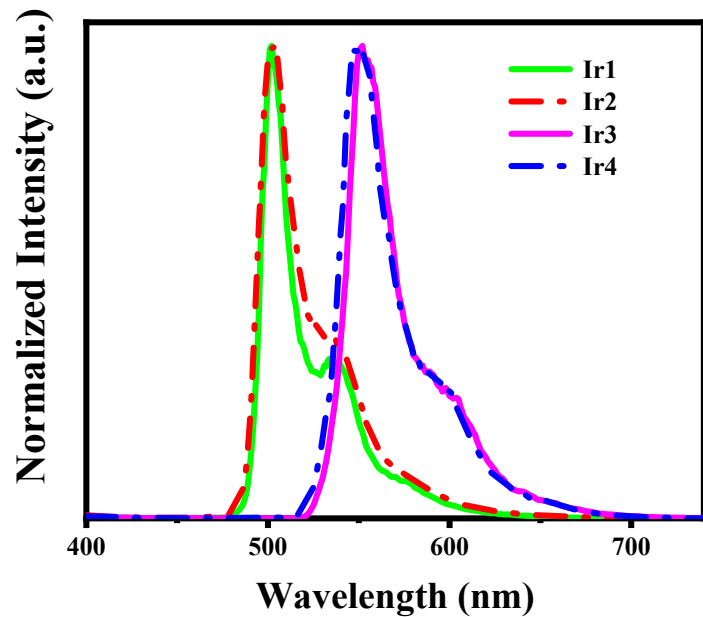
Fig. S18. The 77 K phosphorescent spectra of Ir1-Ir4 in dilute DCM (10^{-5} M).
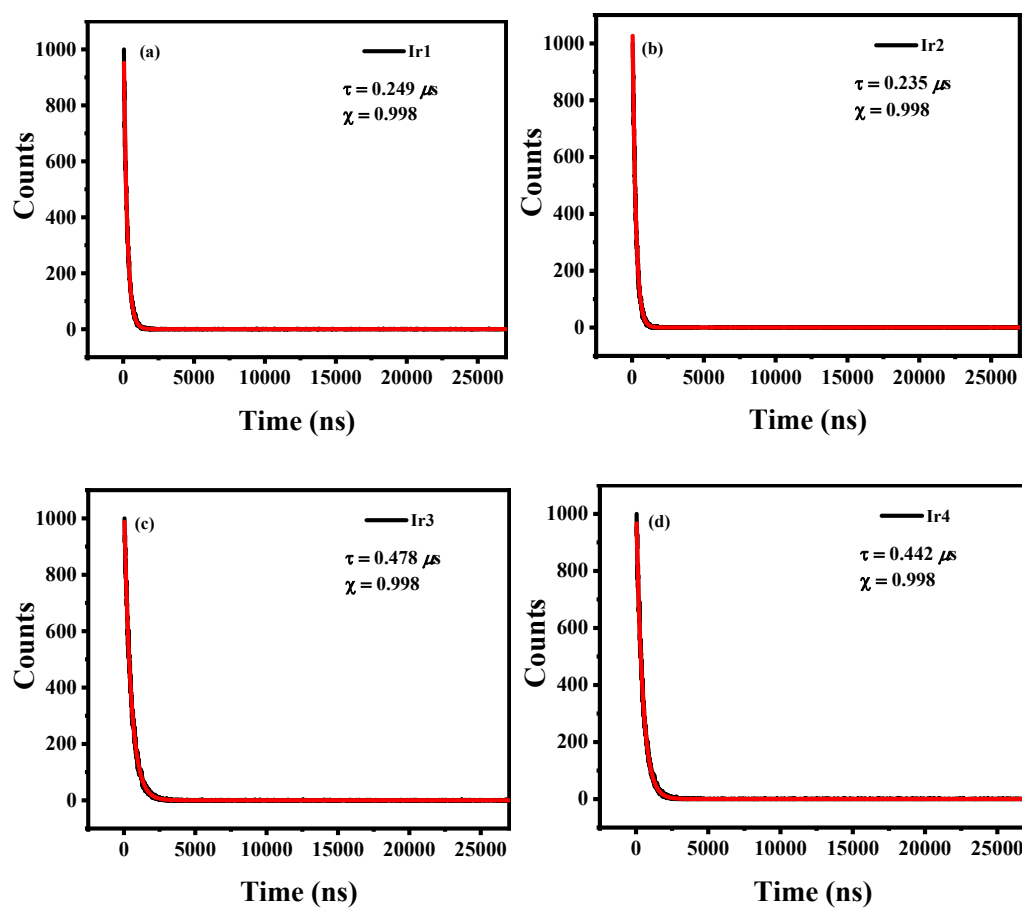
Fig. S19. Phosphorescence lifetime curves of the Ir(III) complexes in dilute DCM (10^{-5} M) at RT.
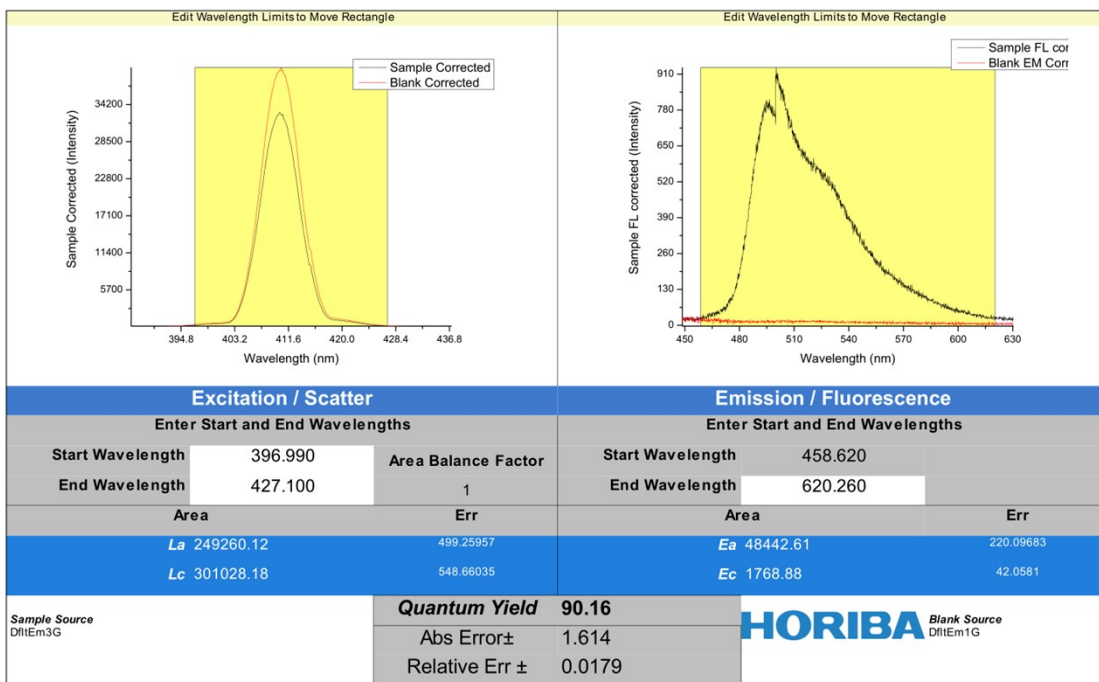
Fig. S20. The photoluminescence quantum yield of Ir1 in the doped film.
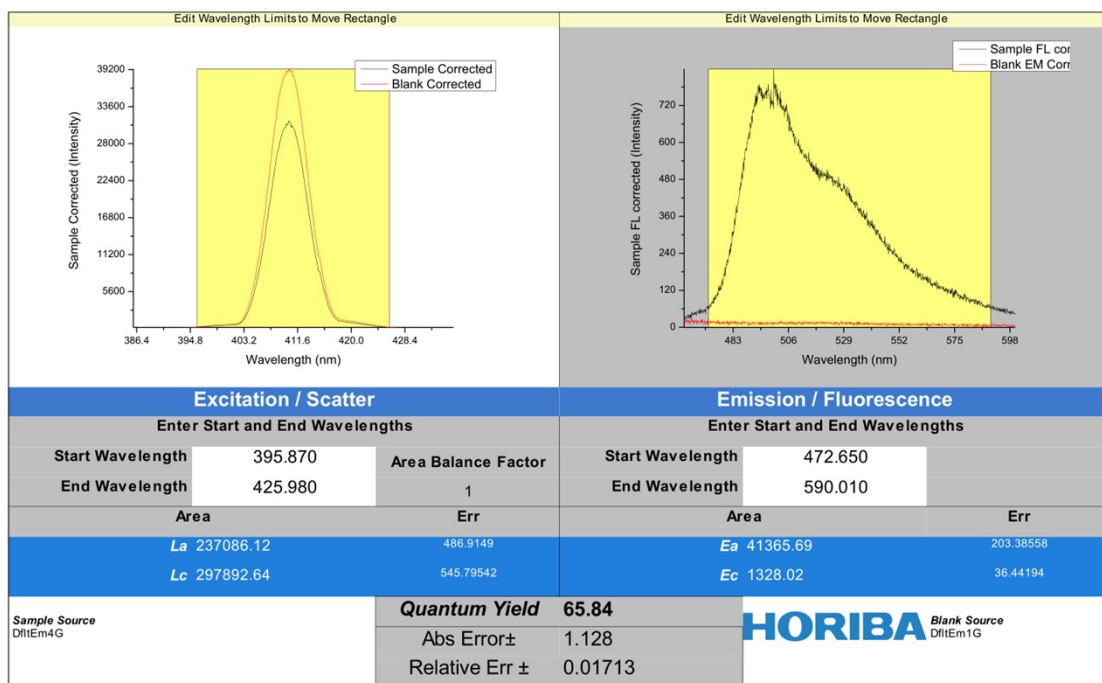
Fig. S21. The photoluminescence quantum yield of Ir2 in the doped film.
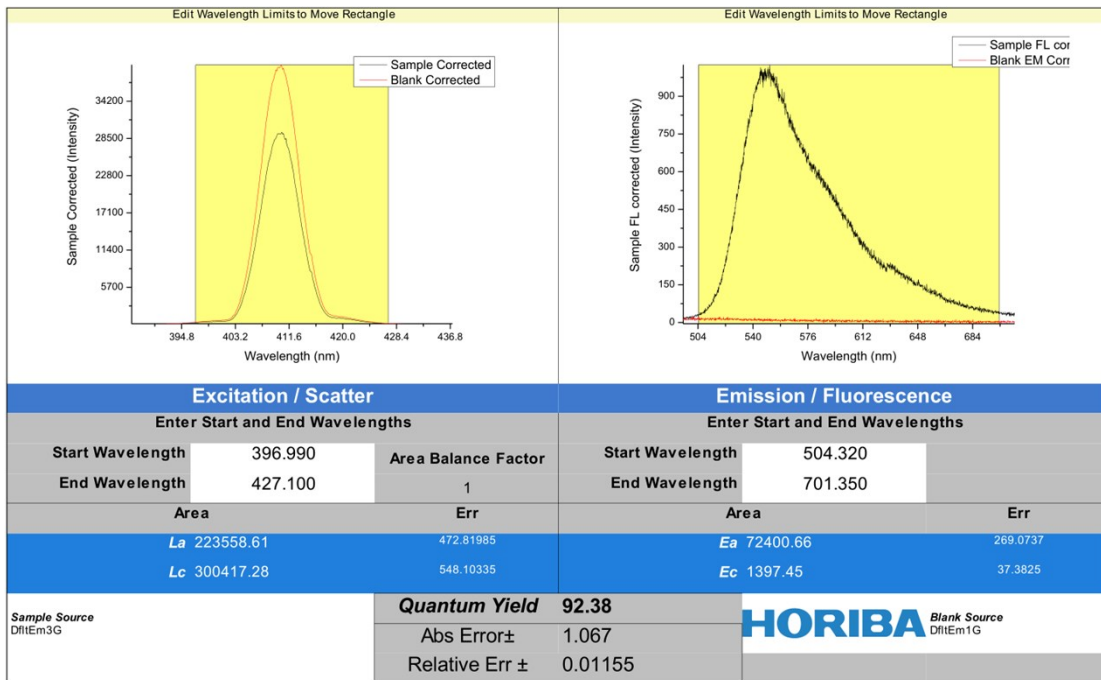
**Fig. S22**. The photoluminescence quantum yield of Ir3 in the doped film.
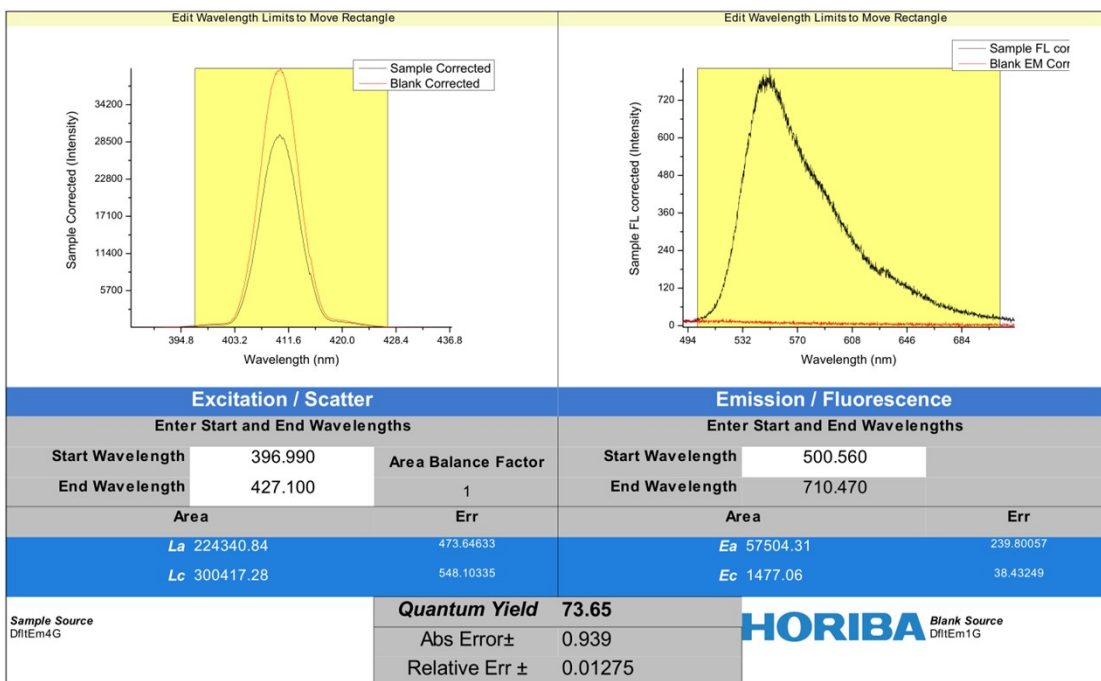
Fig. S23. The photoluminescence quantum yield of Ir4 in the doped film.
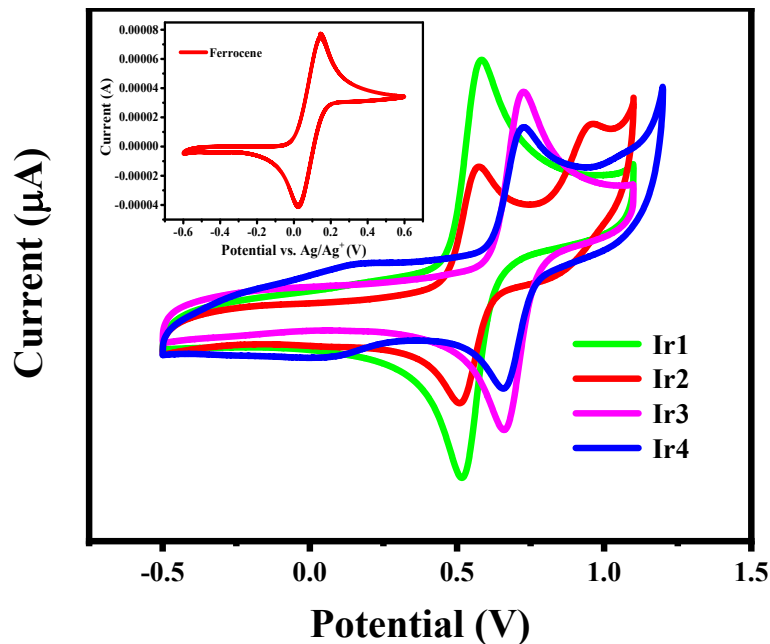
Fig. S24. Cyclic voltammetry curves of the Ir(III) complexes in acetonitrile with ferrocene as the external standard. $E_{Fc+/Fc} = 0.17$ V.
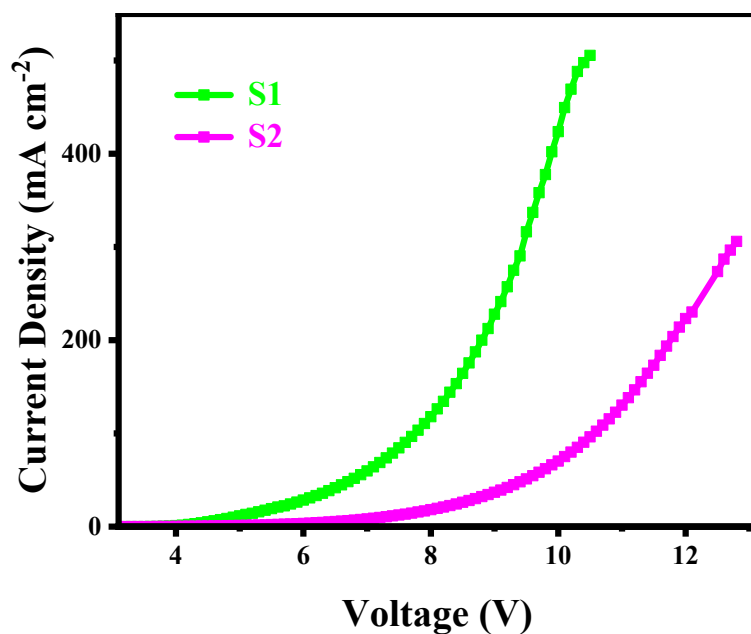

Fig. S25. Current density - voltage curves of devices S1 and S2.

Table S5. Summary of recently reported OLED performances based on Ir(III) complexes vs this work with similar CIE coordinates.

Molecular Structure	CIE (x, y)	EQE$_{max}$ (%)	L_{max} (cd m^{-2})	$\eta_{c,max}$ (cd A^{-1})	REF.
	(0.22, 0.60)	19.8	57185	60.6	*J. Mater. Chem. C*, 2016, **4**, 5469.
	(0.33, 0.62)	26.5	—	91.9	*ACS Appl. Mater. Interfaces*, 2019, **11**, 7184.
	(0.24, 0.58)	23.1	12270	73.9	*Dyes and Pigments*, 2019, **164**, 206.
	(0.34, 0.60)	26.0	89480	—	*Eur. J. Inorg. Chem*, **2018**, 4614
	(0.19, 0.61)	23.8	31318	76.9	This Work
	(0.44, 0.53)	13.5	> 27300	40.7	*ACS Photonics*, 2018, **5**, 3428.
	(0.46,0.53)	18.2	18290	58.5	*Dalton Trans.*, 2020, **49**, 13797.
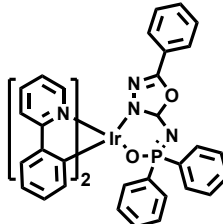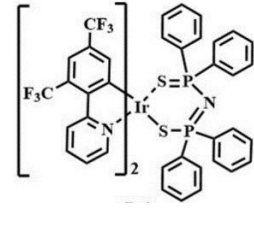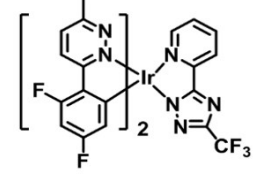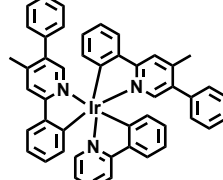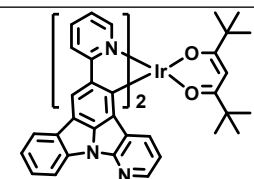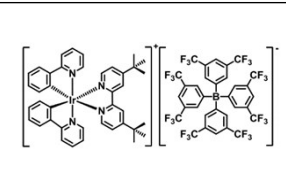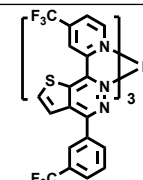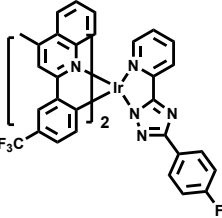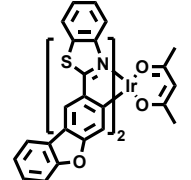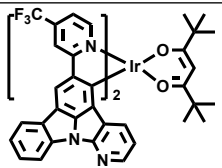
	(0.47, 0.50)	22.7	33571	67.5	*Adv. Funct. Mater.*, 2016, **26**, 881.
	(0.45, 0.52)	19.0	65633	58.4	*ACS Appl. Mater. Interfaces.*, 2013, **5**, 4937.
	(0.46, 0.54)	24.5	33018	87.6	This Work